



Role of nuclear factor-kappa B in bleomycin induced pulmonary fibrosis and the probable alleviating role of ginsenoside: histological, immunohistochemical, and biochemical study

Dalia Refaat El-Bassouny, Nesreen Mostafa Omar, Hanaa Attia Khalaf, Reem Ahmad Abd Al-Salam
Medical Histology and Cell Biology Department, Faculty of Medicine, Mansoura University, El Mansoura, Egypt

Abstract: Bleomycin (BLM) is one of anti-cancerous drugs. One of its limitation is the development of pulmonary fibrosis during therapy. So, we proposed to examine the outcome of BLM take on the light and electron microscopic design of rat lung. Along with, assessment the probable protecting role of ginsenoside on BLM induced pulmonary changes. In this study, thirty adult male albino rats were comprised and were classified to four clusters; Negative & positive control group, BLM treated group and BLM& ginsenoside treated group. The lung was treated for histological and immunohistochemical (anti-p65) studies. Light microscopic examination of H&E stained sections of BLM treated group showed huge distortion of the lung building. Mallory trichrome stain of this group showed evident deposition of collagen fibers in the markedly thickened interalveolar septa and around intrapulmonary bronchi, bronchioles and blood vessels. Moreover, strong positive staining for nuclear factor (NF)- κ B in the wall of bronchiole as well as the thickened interalveolar septa were observed. Ultrastructural inspection of lung of this group revealed muddled lung planning. Marked improvement of the lung structure and marked reduction in NF- κ B immunoexpression was appeared in BLM and ginsenoside treated group. So, we concluded that co-administration of ginsenoside with BLM significantly enhanced the histological and morphometric image of the lung.

Key words: Bleomycin, Ginsenosides, Pulmonary fibrosis, Nuclear factor-kappa B

Received April 7, 2021; Revised June 17, 2021; Accepted August 9, 2021


Introduction

Pulmonary fibrosis is considering a long-standing irrevocable advanced interstitial lung disease with poorly outcome leading to high rates of morbidity and mortality [1]. It is considered to be the most important complication of chemotherapeutic agents [2].

It is accompanying with an average survival rate of not more than 3 years. This disease is characterized by damage of alveolar lining cells, epithelial-mesenchymal transition, activation and accumulation of fibroblasts as well as myofibroblasts leading to increased deposition of extracellular matrix (ECM) within the lung parenchyma [3]. The disease is also associated with infiltration of the lung tissue by many inflammatory cells including neutrophils and eosinophils in association with increased synthesis of connective tissue and inhibition of proteases [4, 5]. These changes lead to complete destruction of the alveolar histoarchitecture ended by respiratory failure [6].

Bleomycin (BLM) is one of anti-cancerous drugs. It is currently used in treating various types of cancers like testic-

Corresponding author:

Hanaa Attia Khalaf 
Medical Histology and Cell Biology Department, Faculty of Medicine,
Mansoura University, El Mansoura 35516, Egypt
E-mail: ok67203964949@yahoo.com

Copyright © 2021. Anatomy & Cell Biology

This is an Open Access article distributed under the terms of the Creative Commons Attribution Non-Commercial License (<http://creativecommons.org/licenses/by-nc/4.0/>) which permits unrestricted non-commercial use, distribution, and reproduction in any medium, provided the original work is properly cited.

ular, prostate, ovarian, breast and cervical tumor. One of the limitations of BLM usage is the development of pulmonary fibrosis during the course of therapy [7-9].

BLM causes oxidative stress, increases the production of pro-inflammatory cytokines and activation of fibroblasts causing complete alteration and damage of pulmonary structures that finally ended by pulmonary fibrosis [10].

The use of herbs in medical purposes is considered as an alternative medicine. Herbs were the main sources of many important drugs and have been the model for many synthetic agents [11, 12].

Ginsenoside is the major bioactive component mined from the root of *Panax ginseng*, which is frequently used in treatment of respiratory, gastrointestinal and cardiovascular diseases [13]. Pharmacological actions of ginsenoside have been confirmed in central nervous system and cancer counting anti-stress and anti-oxidant activities [14].

Ginsenoside has anti-fibrotic, anti-inflammatory, anti-oxidant [15, 16] and anti-tumor effects [17]. Previous studies showed that ginsenoside has immunomodulatory effects that can be used for management of several immune system disorders and also attenuates lung inflammation and prevents the development of pulmonary fibrosis in rats [18, 19].

Many researches were established in the expectation of discovery a treatment that can deliberate disease evolution and hence advance survival of pulmonary fibrosis. However, pulmonary fibrosis remains a challenging disease to manage. As a result, there is an urgent need for new modulators of pulmonary fibrosis which interfere with the pathogenesis of the disease and prevent tissue remodeling [20, 21]. So, we proposed to examine the outcome of BLM take on the light and electron microscopic design of rat lung. Along with, assessment the probable protecting role of ginsenoside on BLM induced pulmonary changes.

Materials and Methods

Chemicals

BLM sulphat (bleocip): Bleomycin sulphate 15 mg ampoule (bleocip) was purchased from Cipla pharmaceutical company (Lower Parel, Mumbai, India).

Ginsenoside (ginseng): Ginsenoside 100 mg capsule (ginseng) was purchased from PHARCO pharmaceuticals Company (Alexandria, Egypt).

Nuclear factor-kappa B (NF- κ B) (p65) rabbit Polyclonal Antibody Kits (catalog no. 14-6731): It was purchased from

Thermo Fisher Scientific Co., Waltham, MA, USA.

Experimental animals

All rats' experimental protocols and procedures were performed authorizing to the international guidelines for the use of laboratory animals and acquired the Mansoura Faculty of Medicine Institutional Research Board (MFM-IRB) approval (with code number: MS/17.07.93). The duration of the experiment was 5 weeks. Thirty adult male albino rats (180–200 g) were involved in this study. Animals were put in plastic coops under hygiene conditions of aeration and temperature with ordinary laboratory nourish and water *ad libitum*. Rats were classified to four clusters.

Group I: negative control group

Included 5 rats, received 0.5 ml of isotonic saline two times/week (by intraperitoneal injection) and normal saline (via orogastric tube) once daily, all for 4 weeks.

Group II: positive control group

Included 5 rats received 0.5 ml of isotonic saline two times/week by intraperitoneal injection followed by 80 mg/kg ginsenoside dissolved in normal saline (via orogastric tube) once daily for 4 weeks [18, 22].

Group III: BLM treated group

Included 10 rats received 0.5 mg of bleomycin sulphate (bleocip ampoule) dissolved in (0.5 ml) isotonic saline injected intraperitoneal (IP) two times/week for four weeks [23].

Group IV: BLM & ginsenoside treated group

Included 10 rats received BLM injection like group III and ginsenoside (in a dose as group II) for one week before BLM injection and then concomitant with BLM injection (for 4 weeks).

Methods

On the day next the latest dosage, rats were deadened with intraperitoneal injection of sodium pentobarbital (40 mg/kg) [24]. The animals were perfused via the left ventricle with 500 ml 10% neutral buffered formalin. The lung was quickly separated and processed for histological and immunohistochemical studies.

Histological study

Left lung were excised and were put in 10% neutral buff-

ered formalin (for fixation) and treated for light microscopic examination. Paraffin block obtained, sectioned (4–5 μm) and stained with hematoxylin and eosin (H&E) stain [25], Mallory's trichrome stain [26].

Immunohistochemical stain

Avidin-biotin complex technique was used [27]. Samples were riding on positively charged slides, deparaffinization and rehydration were performed. Antigen retrieval for uncovering of antigens was performed by heating the sections in 10 mmol/L citrate buffer, (at pH 6) for two cycles. Hydrogen peroxide (3%) for 5 minutes were added to prevent the endogenous peroxidase activity. The sections were incubated for 30 minutes with the primary monoclonal antibody, anti p65 (Thermo Fisher Scientific Co.) at dilution of 1:100 via phosphate buffered saline (PBS). Then, sections were bathed with PBS several times. Biotinylated goat linker was applied to the sections for 30 minutes (Thermo Scientific Co., Cheshire, UK), incubated with the avidin-biotin compound, then with peroxidase substrate solution for 5 minutes to mask the endogenous peroxidase. Counterstain with Mayer's hematoxylin was done. Negative control slides were put under the same circumstances after omitting the 1ry Ab with PBS [25]. Spleen sections used to evaluate the positivity of the tissue sections.

Electron microscopy (TEM)

Small fragments of right lungs were fixed in 2.5% buffered glutaraldehyde then post fixed with osmium tetroxide, dehydrated, cleared and then infiltrated in epoxy resin [28]. Semi-thin sections (cut at 1 μm) were obtained and stained with toluidine blue. Ultrathin sections were sectioned and stained with uranyl acetate and lead citrate then examined using a JEOL transmission electron microscope (100 CX; Tokyo, Japan) at the Faculty of Science, Alexandria University, Alexandria, Egypt.

Computer assisted digital image analysis

Slides were photo'd by Olympus® digital camera (E24-10 M pixel, China) connected to Olympus® microscope with 0.5 X photo adaptor. The outcome pictures were studied on Intel® Core I3® created computer via Video Test Morphology® software (Saint Petersburg, Russia) by a built-in routine for calibrated mechanized item study. We used it to measure width of the interalveolar septa (H&E stained sections), percentage area of collagenous fibers (Mallory trichrome stained

section), percent area of NF- κ B immunoreaction (NF- κ B stained sections) and number of type II pneumocytes (semi-thin sections).

Biochemical study

Lung samples were quickly isolated, perfused with PBS (pH 7.4) and with heparin to eradicate any red blood cells then centrifuge after instantly homogenized in potassium phosphate (pH 7.5). The supernatants were gotten and used for detection of superoxide dismutase (SOD) [29], catalase (CAT) [30], and level of malondialdehyde (MDA) [31].

Statistical analysis

The morphometric data and biochemical were evaluated via the computer program SPSS (statistical package for social science) version 20 (IBM Corp., Armonk, NY, USA). The meaning of difference was tested using ANOVA (Analysis of Variance) followed by post-hoc Tukey for many evaluations. Values are presented as mean \pm SD. *P*-value ≤ 0.05 was considered statistically significant [32].

Results

BLM induced marked distortion of lung architecture and ginsenoside reversed the effects

Light microscopic inspection of lung of control group sections stained with H&E displayed the standard systematized histological building of the lung. The alveoli were inflated (Fig. 1A). The bronchioles mucosa was creased and lined by columnar epithelium. Circular smooth muscle layer lied around the mucosa while adventitia was built of loose connective tissue (Fig. 1A). The intrapulmonary bronchi wall was designed of mucosa, musculosa and adventitia. The mucosa was lined by pseudostratified columnar ciliated epithelium with few goblet cells. The smooth muscle layer was spirally arranged around the mucosa. Adventitia, the outmost coat, exhibited plates of hyaline cartilage with normal chondrocytes some of them formed cell nest (Fig. 1B).

Light microscopic examination of H&E stained sections of BLM treated group revealed huge distortion of the lung building. Most of the alveoli appeared collapsed with few emphysematous ones. The interalveolar septa were markedly thickened with mononuclear cellular infiltration. Obviously dilated, congested and thickened blood vessels were observed (Fig. 1C). The wall of the bronchioles was markedly distorted with appearance of intraluminal cellular debris. The epi-

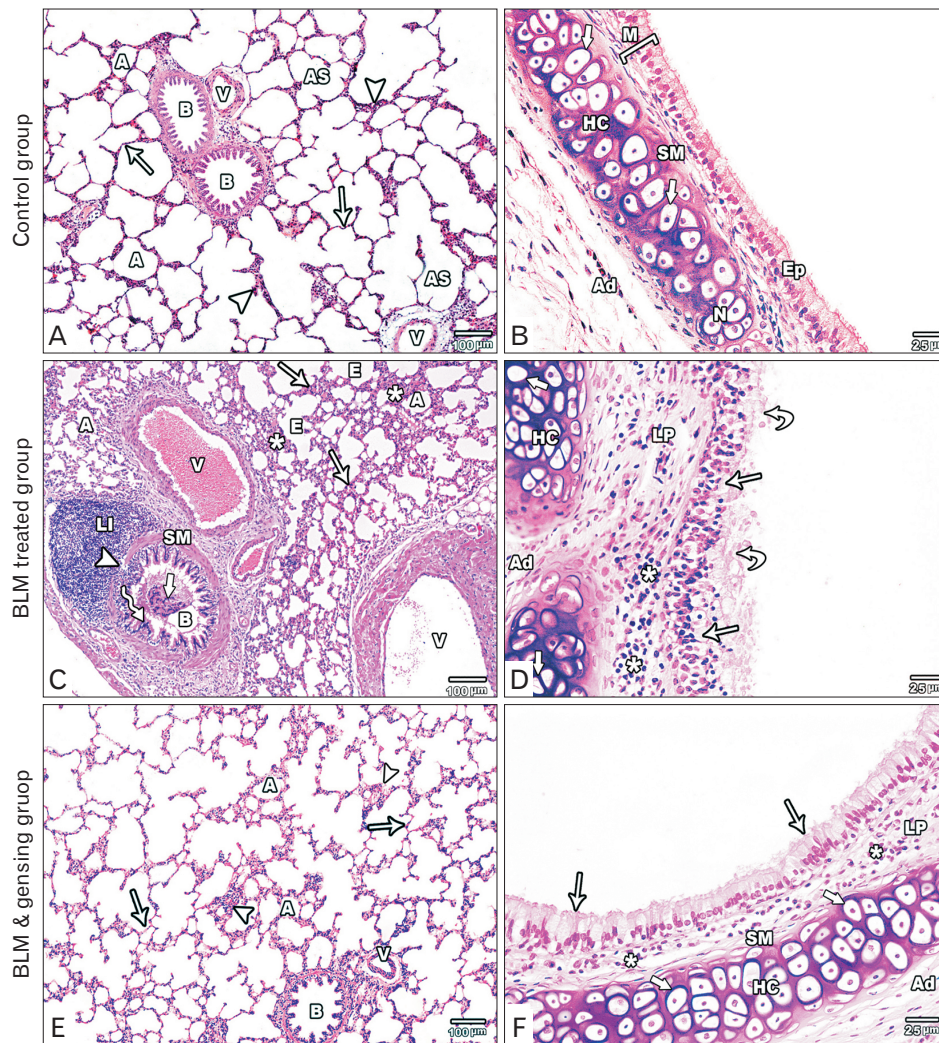


Fig. 1. Figure showed photos of H&E-stained lung sections. (A, B) Control sections: (A) The lung section shows alveoli (A), alveolar sacs (AS), bronchioles (B) with folded mucosa, blood vessels (V), thin (arrows) and thick (arrow heads) portions of the interalveolar septum. (B) The intrapulmonary bronchus is formed of mucosa (M) lined by pseudostratified columnar ciliated epithelium with goblet cells (Ep), is surrounded by smooth muscle layer (SM) and hyaline cartilage (HC) with normal chondrocytes (thick arrow) in the adventitia (Ad). (C, D) Bleomycin (BLM) treated sections: (C) Collapsed alveoli (A) is seen with emphysematous ones (E). It separated by thick interalveolar septa (arrows) with mononuclear cellular infiltration (asterisks). The bronchioles (B) lining epithelium (zigzag arrow) is distorted with the appearance of intraluminal cellular debris (thick arrow), its smooth muscle layer (SM) is thickened and focally interrupted (arrowhead) by massive peribronchiolar lymphocytic infiltration (LI). Note, the presence of congested, thickened and dilated blood vessels (V). (D) Massive distortion and stratification (arrows) of the lining epithelium of the intrapulmonary bronchi with intraluminal cellular debris (curved arrows). Mononuclear cellular infiltration (asterisks) in the lamina propria (LP). Hyaline cartilage (HC) in the adventitia (Ad) is degenerated with absent nuclei of its chondrocyte (thick arrow). (E, F) BLM & ginsenosides treated sections: (E) The lung section shows inflated alveoli (A), intact bronchioles (B) with intact lining and blood vessels (V). The interalveolar septum is thin (arrows) with mild thickened parts (arrow heads). (F) The intrapulmonary bronchi show intact epithelial lining (arrows), mild mononuclear cellular infiltration (asterisks) in the lamina propria (LP). Thin smooth muscle layer (SM) and intact hyaline cartilage (HC) with normal chondrocytes (thick arrows) in the adventitia (Ad). (A, C, E) $\times 100$; (B, D, F) $\times 400$.

thelium showed massive distortion with focal stratification. Smooth muscle layer was thickened and focally interrupted by massive peribronchiolar lymphocytic infiltration (Fig. 1C). The intrapulmonary bronchi showed massive distortion

and thickening of its epithelial lining with focal stratification and intraluminal cellular fragments. Manifested mononuclear infiltration in the lamina propria and adventitia was seen. The cartilage plate in the adventitia showed degeneration of

the chondrocytes with absent nuclei (Fig. 1D).

Light microscopic inspection of H&E stained sections of BLM and ginsenoside treated group exhibited planned lung architecture. Most of the alveoli appeared intact and inflated. The interalveolar septa appeared thin with focal thickenings and mononuclear cellular infiltration. The wall of blood vessels appeared normal (Fig. 1E). Intact epithelial lining of the bronchioles was observed with minimal peribronchiolar cellular infiltration and normal circular smooth muscle layer (Fig. 1E). The wall of the intrapulmonary bronchi appeared intact with normal epithelial lining. Slight mononuclear cel-

lular infiltration was found in the lamina propria and the smooth muscle layer appeared thin. Intact hyaline cartilage plate in the adventitia appeared with normal chondrocytes (Fig. 1F).

BLM induced pulmonary fibrosis and ginsenoside attenuate this effect

Light microscopic inspection of Mallory's trichrome stained sections of control groups showed fine collagen fibers in the interalveolar septa and around intrapulmonary bronchi, bronchioles and blood vessels (Fig. 2A, B). BLM

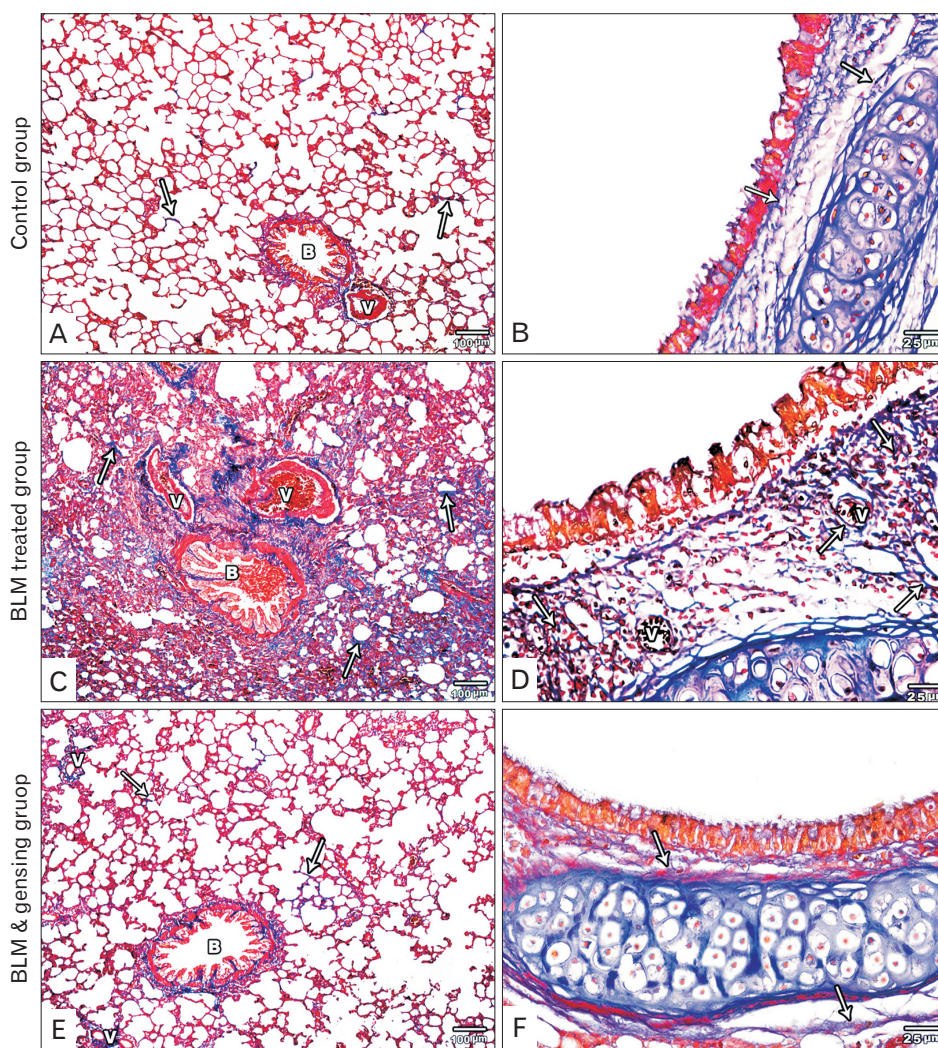


Fig. 2. Figure showed photos of mallory trichrome-stained lung sections. (A, B) Control sections: (A) Fine collagen fibers is observed in the interalveolar septa (arrows), around bronchioles (B) and blood vessels (V). (B) Fine collagen fibers (arrows) is detected in the lamina propria and adventitia of the intrapulmonary bronchi. (C, D) Bleomycin (BLM) treated sections: (C) Massive deposition of collagen fibers in the thickened interalveolar septa (arrows), in the wall of bronchioles (B) and blood vessels (V) and around them. (D) Massive deposition of collagen fibers (arrows) in the lamina propria and adventitia of the intrapulmonary bronchi and around the blood vessel (V). (E, F) BLM & ginsenosides treated sections: (E) Mild deposition of collagen fibers in the interalveolar septa (arrows), around bronchioles (B) and blood vessels (V). (F) Minimal deposition of collagen fibers (arrows) in the lamina propria and adventitia of the intrapulmonary bronchi show. (A, C, E) $\times 100$; (B, D, F) $\times 400$.

treated group showed huge deposition of collagen fibers in the thickened interalveolar septa and around intrapulmonary bronchi, bronchioles and blood vessels (Fig. 2C, D). On the other hand, BLM and ginsenoside treated group showed mild collagen fibers deposition in the interalveolar septa and around intrapulmonary bronchi, bronchioles and blood vessels (Fig. 2E, F).

*BLM increased NF- κ B immunoexpression in the lung
ginsenoside reverse this effect*

Light microscopic examination of anti-NF- κ B stained sections of control groups showed negative immune-expression of NF- κ B in the bronchiole and minimal expression in

the interalveolar septa (Fig. 3A). BLM treated group showed strong positive staining for NF- κ B in the mucosa and adventitia of bronchiole as well as the thickened interalveolar septa (Fig. 3B, C). However, BLM and ginsenoside treated group revealed mild NF- κ B immune-expression in the mucosa and adventitia of bronchiole as well as the interalveolar septa (Fig. 3C).

*BLM increased pneumocyte type II population and
ginsenoside reverse the effect*

Examination of semithin sections of lung of control rats showed inflated alveoli separated by interalveolar septa. These alveoli were lined by type I and type II pneumocytes.

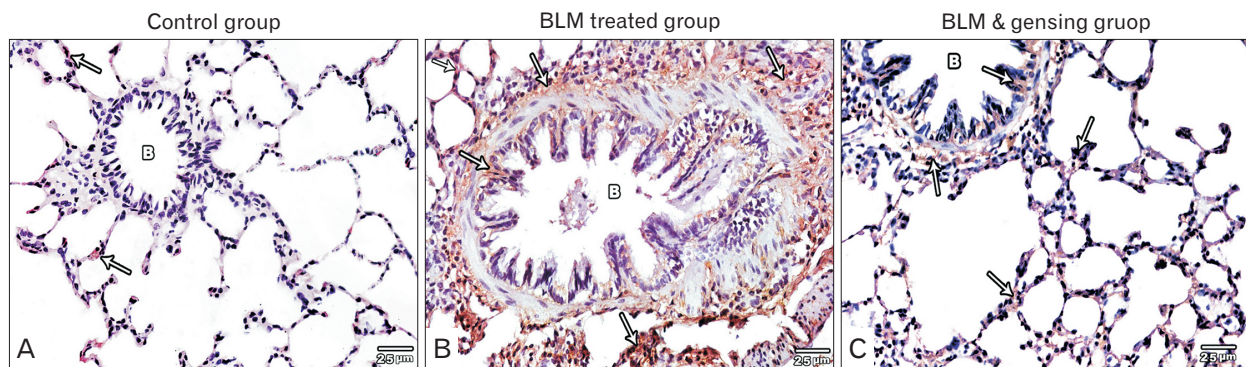


Fig. 3. Figure showed photos of anti-nuclear factor (NF- κ B (anti p⁶⁵) stained lung sections ($\times 400$). (A) Control sections show negative immune-expression of anti NF- κ B stain in the bronchioles (B) and very minimal expression in the interalveolar septa (arrows). (B) Bleomycin (BLM) treated sections show strong positive anti NF- κ B stain expression in the interalveolar septa (arrows) and in the mucosa, musculo- & adventitia (arrows) of the bronchial wall (B). (C) BLM & ginsenosides treated sections show mild anti NF- κ B stain expression in the interalveolar septa (arrows) and in the bronchioles (B).

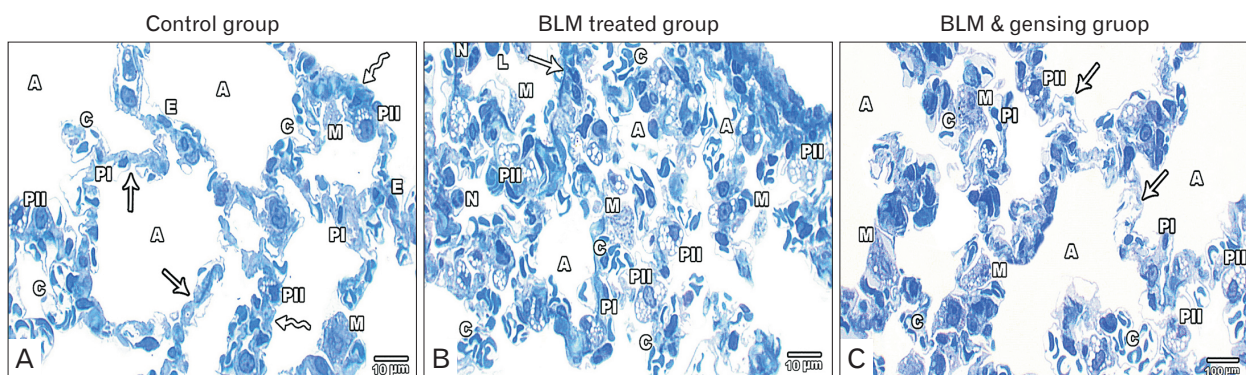


Fig. 4. Figure showed Photos of Semithin stained lung sections ($\times 1,000$). (A) Control sections show lung alveoli (A) lined by type I (PI) and II (PII) pneumocytes. Interalveolar septa is formed of thin (arrows) and thick portions (zigzag arrows) and show few macrophage (M) with the presence of blood capillaries (C) lined by endothelial cells (E). (B) Bleomycin (BLM) treated sections show collapsed alveoli (A), thick septa (arrow) and congested blood capillaries (C). Mononuclear cellular infiltration including alveolar macrophage (M), lymphocytes (L) and neutrophils (N). Few type I pneumocytes (PI) & numerous type II (PII). (C) BLM and ginsenosides treated sections show inflated alveoli (A) lined by type I (PI), II (PII) pneumocytes and some macrophage (M). They are separated by slightly thickened interalveolar septa (arrows) with mild congested blood capillaries (C).

Few alveolar macrophages were seen. Blood capillaries lined by endothelial cells were also seen (Fig. 4A). Semithin sections of the lung of BLM treated group rats showed markedly distorted lung field with collapsed alveoli and thick interalveolar septa. The blood capillaries appeared congested. There was extensive infiltration by inflammatory cells including alveolar macrophages, lymphocytes and neutrophils. Numerous type II pneumocytes were detected (Fig. 4B). Semithin sections of the lung of BLM and ginsenoside treated group showed inflated alveoli with slightly thickened interalveolar

septa. The blood capillaries were mildly congested. Mild increase of type II pneumocytes and some macrophages were observed (Fig. 4C).

BLM induced marked distortion of lung ultrastructure and ginsenoside attenuate this effect

Examination of ultrathin sections of studied groups; showed systematized lung field of the control group. Inflated alveoli were lined by type I and type II pneumocytes. They were disconnected by interalveolar septa (with its thin and

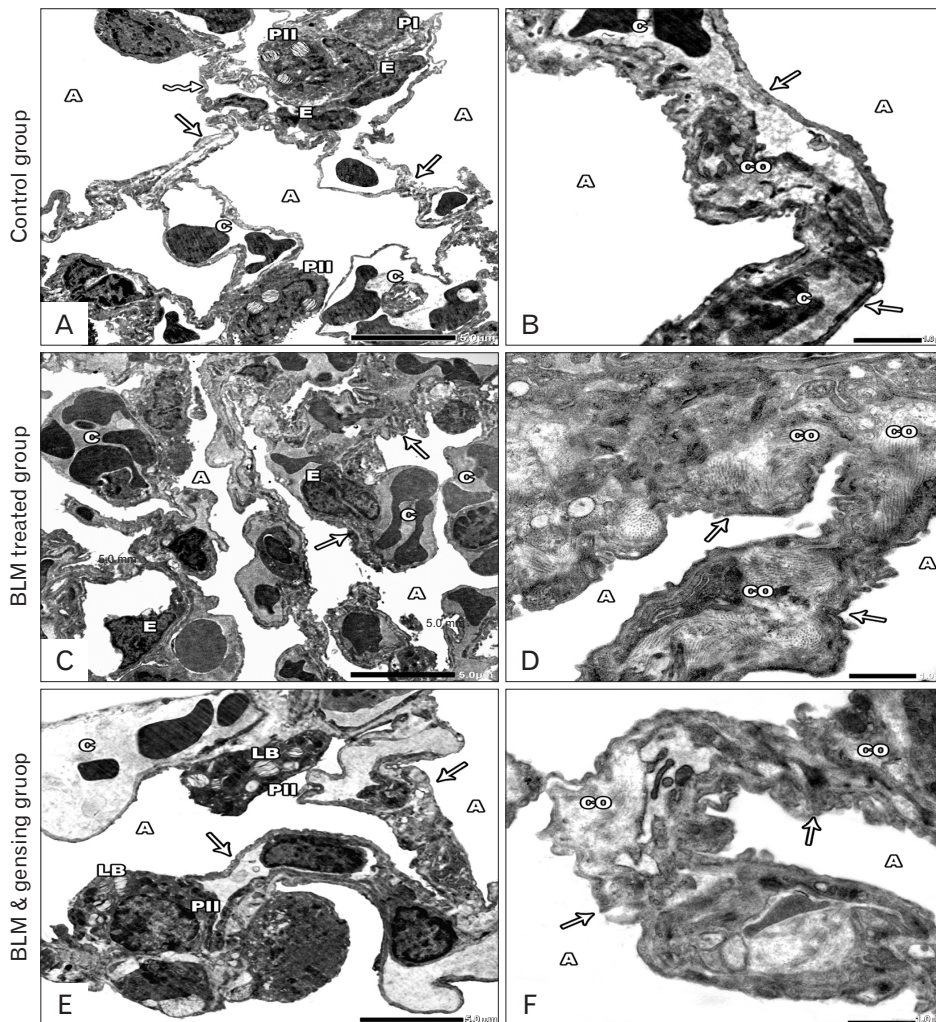


Fig. 5. Photos of ultrathin sections of lung sections. (A, B) Control sections: (A) Lung alveoli (A) are lined by type I (PI) and type II (PII) pneumocytes. The alveoli are separated by interalveolar septa, is formed of thin (arrows) & thick portions (zigzag arrow) with the presence of blood capillaries (C) lined by endothelial cells (E). (B) Lung alveoli (A) separated by interalveolar septa (arrow) with minimal collagen fiber (CO) and blood capillaries (C). (C, D) Bleomycin (BLM) treated sections: (C) Collapsed alveoli (A), thickened interalveolar septa (arrows) with congested blood capillaries (C) and distorted endothelial lining (E) are seen. (D) Collapsed lung alveoli (A) separated by thickened interalveolar septa (arrows) with massive collagen fiber deposition (CO). (E, F) BLM & ginsenosides treated sections: (E) Intact & inflated alveoli (A) separated by thin interalveolar septa (arrows) with mild congested blood capillaries (C). The alveoli are lined by type I (PI) & type II (PII) pneumocytes with its characteristic lamellar bodies (LB). (F) Inflated Lung alveoli (A) separated by interalveolar septa (arrows) with mild collagen fiber (CO) deposition. (A, C, E) $\times 6,000$; (B, D, F) $\times 20,000$.

thick parts) with minimal collagen fiber deposition. The capillaries lined by endothelial cells and contained RBCs (Fig. 5A, B). On the other hand, ultrastructural inspection of BLM treated group revealed muddled lung planning. Most of the alveoli were collapsed with the appearance of cellular debris. The interalveolar septa were markedly thickened with in-

tensive collagen fiber deposition. The blood capillaries were obviously congested with distorted endothelium (Fig. 5C, D). Ultrastructural inspection of lung of BLM and ginsenoside treated group showed noticeable improvement in the lung building. Majority of the alveoli are inflated. The interalveolar septa are thin with mild collagen fiber deposition and

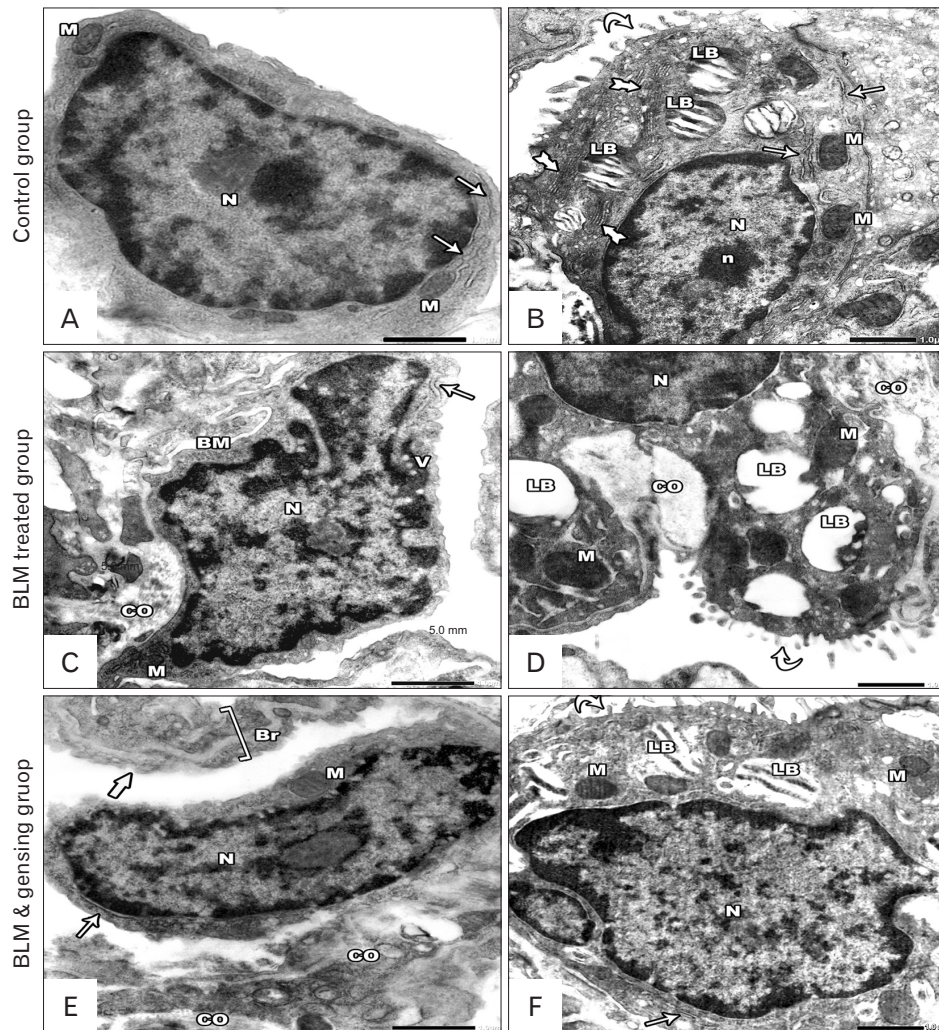


Fig. 6. Photos of ultrathin sections of lung sections. (A, B) Control sections: (A) Type I pneumocyte has large oval euchromatic nuclei (N) and little cytoplasm contain few mitochondria (M) and rough endoplasmic reticulum (rER) (arrows). (B) Type II pneumocyte has large rounded euchromatic nuclei (N) with prominent nucleolus (n) and cytoplasm contain mitochondria (M) and rER (arrows), Golgi apparatus (tailed arrows) and lamellar bodies (LB) with their characteristic closely packed concentric lamellae. It covered by intact short microvilli (curved arrow). (C, D) Bleomycin (BLM) treated sections: (C) Degenerated type I pneumocyte with thickened basement membrane (BM) by collagen deposition (CO), it has irregular nuclei (N) and little cytoplasm contain degenerated mitochondria (M), slightly dilated rER (arrow) and vacuolations (V). (D) Distorted type II pneumocytes with damage of its surface microvilli (curved arrow). It has heterochromatic nucleus (N), its cytoplasm contains degenerated mitochondria (M) with absent cristae, excess collagen fiber deposition (CO) and degenerated lamellar bodies (LB) with loss of its concentric lamellae. (E, F) BLM and ginsenosides treated sections: (E) Type I pneumocyte has large flat regular euchromatic nuclei (N) and little cytoplasm contain few mitochondria (M) and rER (arrow). Thin interalveolar septa (thick arrow) with mild collagen deposition (CO) is seen. Note, the presence of intact blood air barrier (Br). (F) Type II pneumocyte has large rounded euchromatic nuclei (N), its cytoplasm contains intact mitochondria (M) rER (arrow), and lamellar bodies (LB) with their characteristic closely packed concentric lamellae. It covered by intact short microvilli (curved arrow). (A, C, E) $\times 25,000$; (B, D, F) $\times 20,000$.

containing mildly congested blood capillaries (Fig. 5E, F).

Electron microscopic picture of type I pneumocytes of control groups seemed flat and had large oval nuclei. The cytoplasm was contained few organelles as few mitochondria and few cisternae of rough endoplasmic reticulum (rER) (Fig. 6A). Type II pneumocytes of this group appeared cuboidal in shape, bulging into the alveolar lumen with short microvilli covering the cell surface. It had large rounded euchromatic nucleus with prominent nucleoli. Its cytoplasm contained mitochondria, cisternae of rER, saccules of Golgi apparatus and lamellar bodies with the characteristic closely packed concentric lamellae (Fig. 6B). Whereas, type I pneumocytes of BLM treated group were distorted with irregular heterochromatic nuclei. The cytoplasm showed shrunken mitochondria and dilated cisternae of rER with the presence of small vacuolations. Its basement membrane was markedly thickened by the extensive deposition of collagen fibers (Fig. 6C). Type II pneumocytes of this group were damaged with

small irregular and heterochromatic nuclei. The cytoplasm showed electron dense mitochondria with disrupted cristae. The lamellar bodies showed degenerative changes leaving irregular empty vacuoles with loss of the concentric lamellae. The short microvilli covering the cell surfaces were damaged (Fig. 6D). On the other hand, type I pneumocytes seemed intact with euchromatic nuclei and intact organelles (Fig. 6E). Type II pneumocytes appeared slightly intact with large euchromatic nucleus and numerous short microvilli covering the cell surface. Their cytoplasm showed intact organelles and lamellar bodies with the appearance of the characteristic concentric lamellae (Fig. 6F).

Image analysis results and statistical analysis

BLM induced marked thickening of the interalveolar septa and ginsenoside attenuate this effect

The thickness of the interalveolar septa of BLM treated

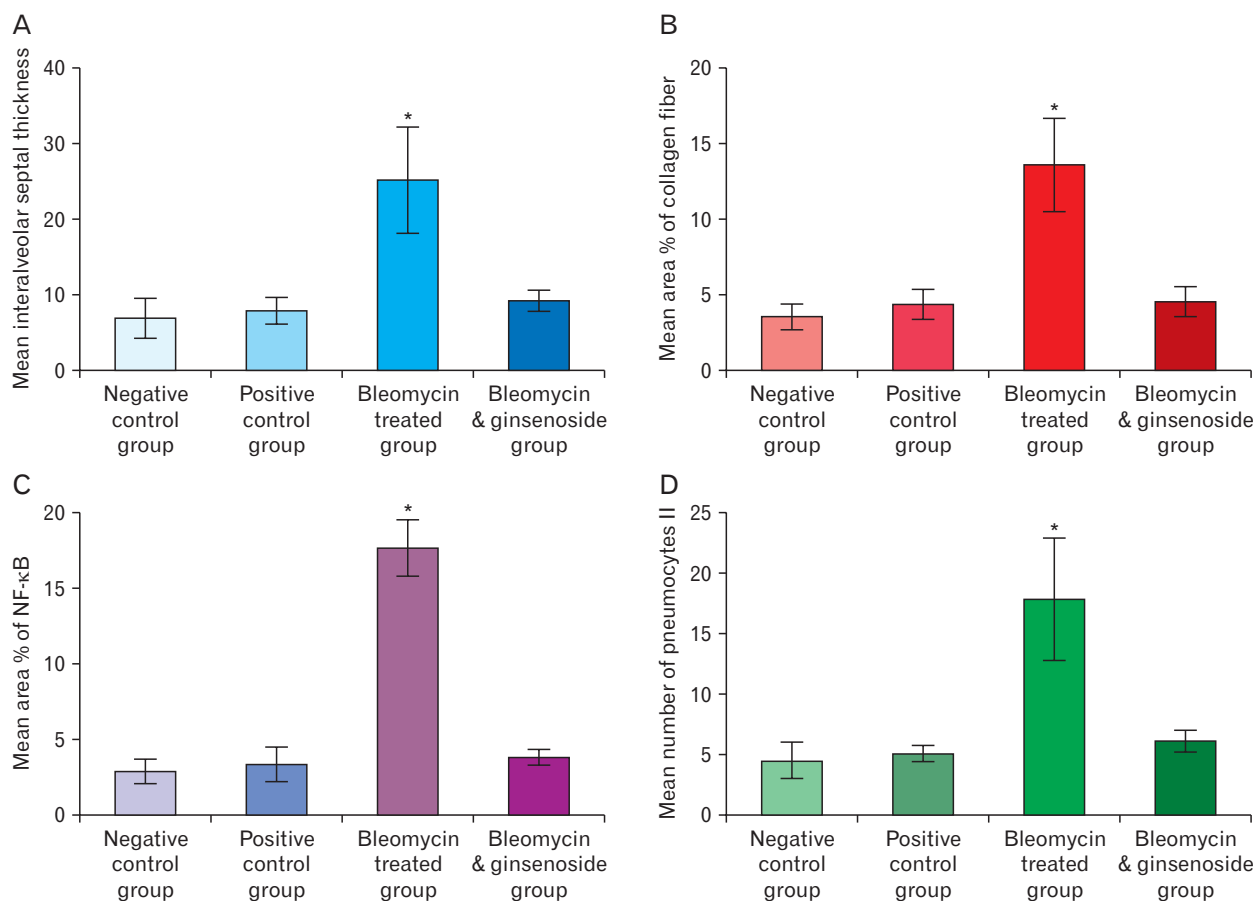


Fig. 7. Morphometric analysis of the studied groups. (A) Thickness of the interalveolar septa of the studied groups. (B) % area of collagen fibers of the studied groups. (C) % area of nuclear factor (NF)-κB immunoreaction of the studied groups. (D) Mean number of type II pneumocytes of the studied groups. *Statistically significant ($P < 0.0001$).

group showed highly significant increase when matched with that of control group ($P<0.0001$); and highly significant decrease when matched with that of BLM and ginsenoside treated group ($P<0.0001$) (Fig. 7A).

BLM induced marked increased in the % area of the collagen fibers and ginsenoside attenuate this effect: (Mallory's trichrome stained sections)

The percentage area of the collagen fibers of BLM treated group showed highly significant increase when matched with that of control group ($P<0.0001$); and highly significant decrease when matched with that of BLM and ginsenoside treated group ($P<0.0001$) (Fig. 7B).

BLM induced marked increased in the % area of the positive reaction in NF- κ B immunohistochemical stained sections and ginsenoside attenuate this effect

The percentage area of positive NF- κ B immune reaction of BLM treated group showed highly significant increase

when matched with that of control group ($P<0.0001$); and highly significant decrease when matched with that of BLM and ginsenoside treated group ($P<0.0001$) (Fig. 7C).

BLM induced marked increase in the number of type II pneumocytes and ginsenoside attenuate this effect

The mean number of types II pneumocytes of BLM treated group showed highly significant increase when matched with that of control group ($P<0.0001$); and highly significant decrease when matched with that of BLM and ginsenoside treated group ($P<0.0001$) (Fig. 7D).

BLM induced marked changes in the oxidative stress markers and ginsenoside attenuate this effect

A highly significant increase in the MDA ($P<0.0001$) and high significant decrease of other oxidative stress markers (CAT, SOD) levels ($P<0.0001$) in the lung tissue of BLM treated group were detected when matched with that of control group. While, a high significant decrease of MDA ($P<0.0001$)

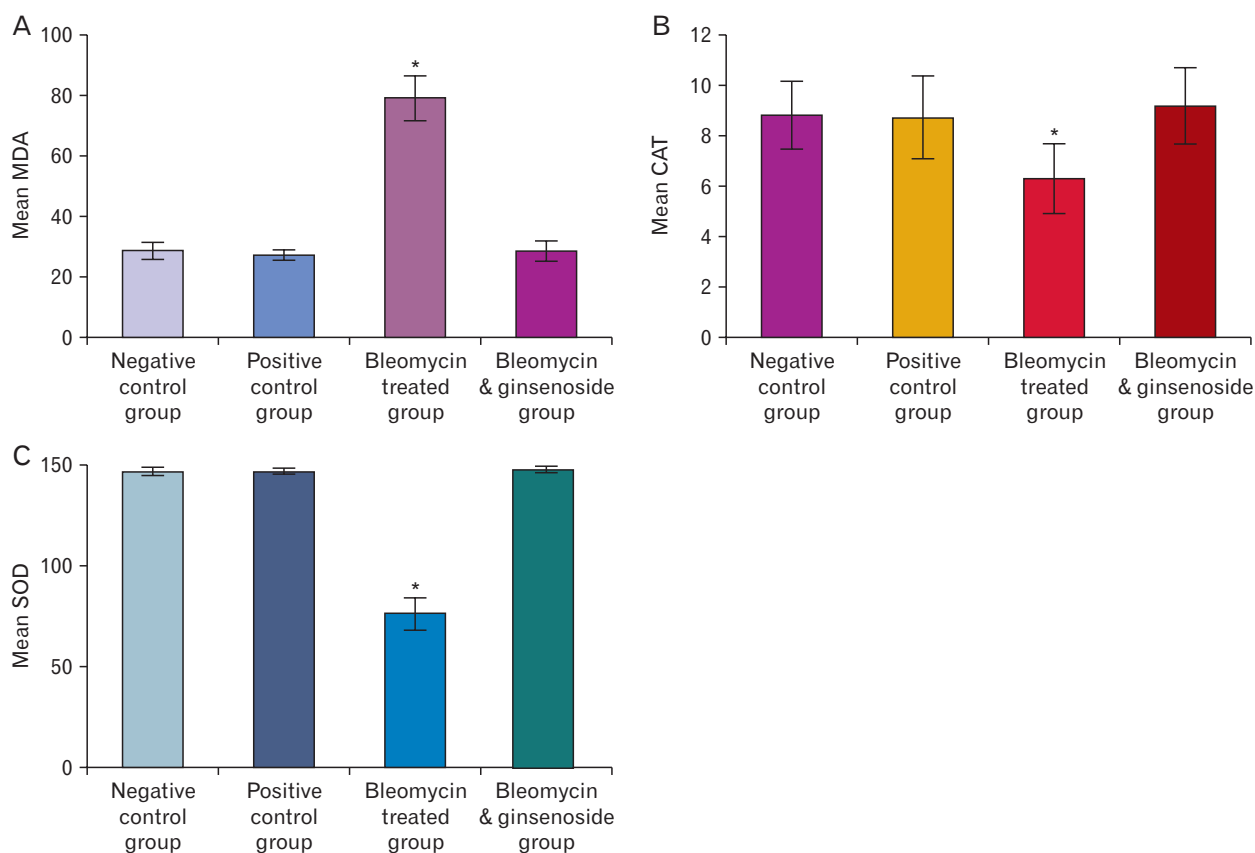


Fig. 8. Oxidative markers of the studied groups. (A) Mean malondialdehyde (MDA) levels in the lung tissue of the studied groups. (B) Mean catalase (CAT) levels in the lung tissue of the studied groups. (C) Mean superoxide dismutase (SOD) levels in the lung tissue of the studied groups. *Statistically significant ($P<0.0001$).

and highly significant increase in CAT, SOD ($P < 0.0001$) were also detected when matched with that of BLM and ginsenoside treated group (Fig. 8).

Discussion

BLM is a commonly used chemotherapeutic agent. It is either used as a single agent or in combinations with other chemotherapeutic agents. BLM causes massive lung injury and fibrosis. The animal model of lung fibrosis induced by BLM resembles what occurs in human, so it is used in studying the mechanisms which cause rapid progression of the disease [33-35].

Ginseng has anti-inflammatory and antioxidant actions. It protects against lung injury and fibrosis so improves lung functions [36]. Consequently, the existing work tried to assess the probable protective role of ginsenosides in BLM induced lung fibrosis.

In the current study, four weeks of BLM administration resulted in massive pulmonary changes. Majority of lung alveoli were collapsed with some emphysematous ones. The interalveolar septa were markedly thickened with evident mononuclear cellular infiltrations. Such findings coincide with those observed by Altintas et al. [37] and Tian et al. [38]. The thickening of interalveolar septa was statistically confirmed and coincides with that found by Tang et al. [39].

This noticeable thickening may be due to increased deposition of collagen fibers which is confirmed by Mallory trichrome stained sections and statistically by the high significant rise in the percentage area of collagen fiber matched with that of control rats. Moreover, this thickening may be the cause of collapsed alveoli. Additionally, collapsed alveoli may be also due to vascular congestion and depletion of the pulmonary surfactant [40, 41]. However, the presence of dilated alveoli could be result of epithelial, endothelial and basement membrane damage [42, 43].

The intrapulmonary bronchi and bronchioles of BLM administrated group showed marked distortion in their walls with thickening of their smooth muscle layer and extensive mononuclear cellular infiltration with degeneration of the chondrocytes of the hyaline cartilage plate. These changes are consistent with that of [44, 45].

Liu et al. [46] reported that the production of inflammatory agents as transforming growth factor beta (TGF- β) and tumor necrotic factor alpha (TNF- α) has a vital role in the proliferation and thickening of smooth muscle layer. Zaafan

et al. [47] stated that BLM initiates oxidative stress with consequent increased production of reactive oxygen and nitrogen species. These oxidants stimulate many genes associated with cell growth and cell death. BLM also increases the production of pro-inflammatory agents as interleukin (IL)-6 and proteolytic enzymes leading to lipid peroxidation of the cell and defect in synthesis and degradation of lung prostaglandins [37, 48].

The degenerative changes of hyaline cartilage caused by BLM were mainly due to oxidative stress that lead to increase of COX-2 and prostaglandin E2 in chondrocytes causing its damage [49]. As well as, some cytokines as TNF- α , IL1 act by promoting inflammatory responses and encouraging cartilage damage [50].

Thickening of the blood vessels wall and extravasation of RBCs may be due to deviations in the vascular integrity of the lung capillary leading to damage of the endothelial barrier and impairment in capillary permeability [23, 51, 52].

Massive deposition of collagen fibers was detected in BLM administrated group around the alveoli, intrapulmonary bronchi, bronchioles, and blood vessels. These data come in line with [53, 54].

It is believed that BLM causes injury to the alveolar epithelium and its basement membrane; which is an essential step in the etiology of lung fibrosis. This injury leads to fibroblasts proliferation, marked increase in collagen deposition and accumulation of ECM proteins. As a result, interstitial edema, hemorrhage and thickened interstitium of the alveoli occur resulting in breakdown of connective tissue giving the picture of emphysema [48, 55, 56]. Moreover, many inflammatory cells migrate to and proliferate in sites of damage. These cells produce many cytokines causing more cell staffing and remodeling of matrix leading to excessive production of collagen and matrix components [57, 58]. Also, several inflammatory cytokines; especially TGF- β ; are produced from the destructed lung tissue mainly through the activation of NF- κ B pathway leading to production of fibroblasts [47, 48].

TGF- β can be secreted in the lung via many cells (macrophages, alveolar epithelial cells, endothelial cells, fibroblasts, as well as myofibroblasts). When activated, TGF- β leading to recruitment and proliferation of both macrophage and fibroblast [59, 60], causing more collagen deposition [55, 61].

Four weeks of BLM administration give rise to over expression of NF- κ B in the lung tissue of the current work. This was confirmed by the high significant rise in the per-

centage area of positive immune reaction in the lung of BLM treated group matched with control groups. Similar results were obtained by Kabel et al. [62].

NF- κ B is a member of dimeric DNA binding transcription agents. It modifies the vital responses to cellular stress via the regulation of effector genes expression [63]. It is present in the cytoplasm of every cell and when activated translocate to the nucleus. Its activation is induced by free radical-sand toxins. Once it is activated, it regulates the expression of genes of several inflammatory agents as enzymes (COX-2 and iNOS) and many mediators (IL-1B, IL-6, TNF- α , and TGF- β), which are extremely related with the development of pulmonary fibrosis, especially TGF- β [64-66].

Toll like receptor 4 (TLR-4) is a crucial manager of the pro-inflammatory transcript NF- κ B factor. Stimulation of TLR-4 signaling in fibroblasts give rise to increased collagen deposition and enhanced expression of several genes tangled in tissue repair and ECM [54].

NF- κ B changes cell behavior in many ways; it regulates the transcription of large number of genes, especially those involved in immune and inflammatory responses and thus has a role in regulating inflammation, cell proliferation and apoptosis [64, 67]. Also, it acts as a significant controller of many functions including cellular proliferation; especially fibroblast; inflammation and differentiation [68, 69].

Many evidences showed that NF- κ B signaling pathway can be activated by BLM and plays an important role in controlling inflammation [39, 38]. As well as it has an important role in BLM-induced pulmonary fibrosis [68, 69].

In the current work, semi thin sections of BLM treated group revealed marked rise in the quantity of types II pneumocytes and it was confirmed statistically. This could be attributed to destruction of type I pneumocytes with its replacement by the proliferating type II pneumocytes as the majority of the alveolar lining, type I pneumocytes, are more susceptible to injury induced by BLM [23]. Cellular infiltration with inflammatory cells was also recorded. It was reported that many inflammatory cells are involved in different stages of lung fibrosis [70].

Macrophages are the chief cells elaborated in BLM administration. They produce IL-7 which has principle action in pulmonary fibrosis [71]. Also, it has essential role in all phases of fibrosis via its extraordinary flexibility for adaptation to definite stimuli [57, 72].

In the present research, ultrastructural inspection of lung sections of BLM treated group revealed markedly thickened

interalveolar septa with extensive deposition of collagen fibers and inflammatory cells infiltration. The alveoli were collapsed with the appearance of intra luminal cellular debris. Similar change was obtained by Kandhare et al. [73], Zhao et al. [74], and Zhou et al. [75].

Structural changes in both pneumocyte types were noted in the form of irregular nucleus, degenerated organelles, and cytoplasmic vacuolation in addition to degenerated lamellar bodies with loss of its concentric lamellae leaving irregular empty vacuoles. Similar observations were also recorded by others [23, 73].

Degenerative changes of organelles are explained by Hüttemann et al. [76], Liu and Chen [77] and Burman et al. [78] as adaptive processes to unfavorable conditions as excessive exposure to free radicals and hypoxia. The stressed mitochondria release cytochrome C which in turn activates caspase-9 initiating irreversible phases of apoptosis. This causes an increase in the lipid peroxidation and activation of the intrinsic pathway of apoptosis.

The cytoplasmic vacuolations might be due to the release of free radicals which alter Na/K pump role causing accumulation of sodium and migration of water to the cell. Moreover, any toxic agents may be aggregated in the form of vacuoles in the cell [79].

Changes of type II pneumocytes were linked with reduced production and release of lung surfactant as well as change in its composition and function. This defect could be attributed to ROS. The change in surfactant alters the pulmonary surface tension and lead to collapsed alveoli [23, 74].

The current work showed highly significant changes in the oxidative marker in lung tissue of BLM treated group; there was significant rise in level of MDA equivalent with a significant reduction of SOD and CAT levels matched with that of control groups. These data theorized the existence of oxidative stress in BLM treated group and it come in agreement with preceding studies [38, 80, 81].

In the existing work, lung sections of BLM and ginseng treated group showed marked improvement in lung structure more or less similar to that of control groups. The interalveolar septa were intact and thin with normal and inflated alveoli. Statistically there was high significant reduction in the thickness of the interalveolar septa of this group matched with that of BLM treated group. The epithelium of the intrapulmonary bronchi and bronchioles appeared intact with thin smooth muscle layer and minimal mononuclear cellular infiltration in the adventitia. The hyaline cartilage plate in

the adventitia appeared intact with normal chondrocytes. Similar results were obtained by Guan et al. [19] and Gao et al. [82].

In BLM and ginseng treated group, Mallory's trichrome stained sections revealed minimal collagen fibers deposition in the interalveolar septa and around intrapulmonary bronchi, bronchioles and blood vessels. Statistically highly significant reduction in the percentage area of collagen fibers matched with that of BLM treated group. Similar results were run with that published by Zhou et al. [83].

Mild positive immune expression for NF- κ B in BLM and ginseng treated group was detected and exhibited a high significant reduction matched with BLM treated group. These data come in line with Shergis et al. [13], Saba et al. [84] and Ahn et al. [85].

Improvement of lung field with few inflammatory cells and less frequent type II pneumocytes was detected in semi-thin sections of the lung of BLM and ginseng treated group. This was confirmed by high significant reduction in the mean number of types II pneumocytes in BLM and ginseng treated group when compared with that of BLM treated group rats. This reduction may be caused by the protective effect of ginseng which prevents the damage of type I pneumocytes and preserves their structure and number and thus prevents proliferation of type II pneumocytes.

Remarkably improvement of the lung building of BLM and ginseng treated group was also detected by electron microscopy. The lung design was conserved; the alveoli were inflated with thin interalveolar septa. Similar results were reported by Bilgin et al. [33]. Type I and type II pneumocytes appeared intact. Type II pneumocytes showed intact lamellar bodies with their concentric lamellae. The cytoplasm showed intact organelles. Similar findings were reported by Ren et al. [86].

Ginseng has many pharmacologically bioactive ingredients including ginsenosides, polysaccharides, polyacetylenes, phytosterols, and essential oils. Ginsenosides are the chief active ingredients [87]. Ginsenosides have powerful antioxidant and anti-inflammatory properties via scavenging free radicals and upregulation of antioxidant enzymes. Ginseng regulates inflammation through inhibition of lung pathological changes including edema, cellular infiltration and the release of inflammatory agents (TNF- α , TGF- β , IL-1 β , IL-4, and IL-6) [36, 88].

Many studies have shown that ginseng inhibits lipid peroxidation and NF- κ B activation. The pathogenesis of fibrosis

mediated by many inflammatory agents (mainly TGF- β) which can be inhibited by ginseng [89].

It was also reported that ginseng inhibit lipid peroxidation, ameliorate the endothelial NO thus enhance endothelial dysfunction [90].

Ginsenosides inhibit NF- κ B activation and thus prevent IL-1 β -produced chondrocytes apoptosis and inflammation. The pro-inflammatory cytokine IL-1 β has been proved to reduce chondrocytes viability, up-regulation of pro-apoptotic proteins and activates NF- κ B signaling pathway [91]. Moreover, previous reports have indicated that ginsenosides inhibit TNF- α -induced NF- κ B activation [92].

The current work showed highly significant reduction in lung level of MDA equivalent with a significant rise of SOD and CAT levels in BLM and ginseng treated group matched with that of BLM treated group. These data consistent with Duguran et al. [93] who studied the antioxidant defensive potential of ginseng. It was manifested by a decrease in ROS which is the major contributor to oxidative stress which causes tissue damage by lipid peroxidation. This increase in lipid peroxidation was normalized or decreased by the intake of ginseng.

So, we can concluded that, ginsenosides expressively ameliorated BLM-induced pulmonary fibrosis through the inhibition of NF- κ B activation in addition to their antifibrotic, antioxidant and anti-inflammatory activities. So, ginseng may be a meaningful adjuvant treatment with BLM to eliminate the hazardous of pulmonary fibrosis. Further studies are required to declare the possible mechanisms by which ginseng could mitigate BLM induced pulmonary fibrosis.

ORCID

Dalia Refaat El-Bassouny:

<https://orcid.org/0000-0002-3884-1265>

Nesreen Mostafa Omar:

<https://orcid.org/0000-0001-7483-4030>

Hanaa Attia Khalaf:

<https://orcid.org/0000-0001-6644-5422>

Reem Ahmad Abd Al-Salam:

<https://orcid.org/0000-0001-7013-6462>

Author Contributions

Conceptualization: DREB. Data acquisition: RAAAS. Data analysis or interpretation: NMO, HAK. Drafting of

the manuscript: DREB, NMO, HAK. Critical revision of the manuscript: DREB, NMO, HAK. Approval of the final version of the manuscript: all authors.

Conflicts of Interest

No potential conflict of interest relevant to this article was reported.

References

- Albera C, Costabel U, Fagan EA, Glassberg MK, Gorina E, Lancaster L, Lederer DJ, Nathan SD, Spirig D, Swigris JJ. Efficacy of pirfenidone in patients with idiopathic pulmonary fibrosis with more preserved lung function. *Eur Respir J* 2016;48:843-51.
- Liu Y, Lu F, Kang L, Wang Z, Wang Y. Pirfenidone attenuates bleomycin-induced pulmonary fibrosis in mice by regulating Nrf2/Bach1 equilibrium. *BMC Pulm Med* 2017;17:63.
- Cui Y, Jiang L, Yu R, Shao Y, Mei L, Tao Y. β -carboline alkaloids attenuate bleomycin induced pulmonary fibrosis in mice through inhibiting NF-kb/p65 phosphorylation and epithelial-mesenchymal transition. *J Ethnopharmacol* 2019;243:112096.
- Stoll P, Wuertemberger U, Bratke K, Zingler C, Virchow JC, Lommatzsch M. Stage-dependent association of BDNF and TGF- β 1 with lung function in stable COPD. *Respir Res* 2012;13:116.
- Choi SM, Jang AH, Kim H, Lee KH, Kim YW. Metformin reduces bleomycin-induced pulmonary fibrosis in mice. *J Korean Med Sci* 2016;31:1419-25.
- Wang M, Zhang J, Song X, Liu W, Zhang L, Wang X, Lv C. Astaxanthin ameliorates lung fibrosis *in vivo* and *in vitro* by preventing transdifferentiation, inhibiting proliferation, and promoting apoptosis of activated cells. *Food Chem Toxicol* 2013;56:450-8.
- Peng R, Sridhar S, Tyagi G, Phillips JE, Garrido R, Harris P, Burns L, Renteria L, Woods J, Chen L, Allard J, Ravindran P, Bitter H, Liang Z, Hogaboam CM, Kitson C, Budd DC, Fine JS, Bauer CM, Stevenson CS. Bleomycin induces molecular changes directly relevant to idiopathic pulmonary fibrosis: a model for "active" disease. *PLoS One* 2013;8:e59348.
- Yao Y, Wang Y, Zhang Z, He L, Zhu J, Zhang M, He X, Cheng Z, Ao Q, Cao Y, Yang P, Su Y, Zhao J, Zhang S, Yu Q, Ning Q, Xiang X, Xiong W, Wang CY, Xu Y. Chop deficiency protects mice against bleomycin-induced pulmonary fibrosis by attenuating M2 macrophage production. *Mol Ther* 2016;24:915-25.
- Gerson SL, Caimi PF, William BM, Creger RJ. Pharmacology and molecular mechanisms of antineoplastic agents for hematologic malignancies. In: Hoffman R, Benz EJ, Silberstein LE, Heslop H, Weitz J, Anastasi J, Salama ME, Abutalib SA, editors. *Hematology: Basic Principles and Practice*. 7th ed. Philadelphia: Elsevier Health Sciences; 2018. p.849-912.
- Shariati S, Kalantar H, Pashmforoosh M, Mansouri E, Khodayar MJ. Epicatechin protective effects on bleomycin-induced pulmonary oxidative stress and fibrosis in mice. *Biomed Pharmacother* 2019;114:108776.
- Ballington DA, Anderson RJ. *Pharmacy practice for technicians*. 5th ed. St. Paul: Paradigm Publishing; 2014.
- Jamshidi-Kia F, Lorigooini Z, Amini-Khoei H. Medicinal plants: Past history and future perspective. *J Herbm Pharm* 2018;7:1-7.
- Shergis J, Di Y, Zhang A, Vlahos R, Helliwell R, Ye J, Xue CC. Therapeutic potential of Panax ginseng and ginsenosides in the treatment of chronic obstructive pulmonary disease. *Complement Ther Med* 2014;22:944-53.
- Niranjana Murthy H, Dandin VS, Yoeup Paek K. Hepatoprotective activity of ginsenosides from Panax ginseng adventitious roots against carbon tetrachloride treated hepatic injury in rats. *J Ethnopharmacol* 2014;158 Pt A:442-6.
- Bao S, Zou Y, Wang B, Li Y, Zhu J, Luo Y, Li J. Ginsenoside Rg1 improves lipopolysaccharide-induced acute lung injury by inhibiting inflammatory responses and modulating infiltration of M2 macrophages. *Int Immunopharmacol* 2015;28:429-34.
- Nguyen CT, Luong TT, Lee SY, Kim GL, Kwon H, Lee HG, Park CK, Rhee DK. Panax ginseng aqueous extract prevents pneumococcal sepsis *in vivo* by potentiating cell survival and diminishing inflammation. *Phytomedicine* 2015;22:1055-61.
- Wang CZ, Anderson S, DU W, He TC, Yuan CS. Red ginseng and cancer treatment. *Chin J Nat Med* 2016;14:7-16.
- Chen J, Feng X, Huang Q. Modulation of T-Bet and GATA-3 expression in experimental autoimmune thyroiditis rats through ginsenoside treatment. *Endocr Res* 2016;41:28-33.
- Guan S, Liu Q, Han F, Gu W, Song L, Zhang Y, Guo X, Xu W. Ginsenoside Rg1 ameliorates cigarette smoke-induced airway fibrosis by suppressing the TGF- β 1/Smad pathway *in vivo* and *in vitro*. *Biomed Res Int* 2017;2017:6510198.
- Behr J. The diagnosis and treatment of idiopathic pulmonary fibrosis. *Dtsch Arztebl Int* 2013;110:875-81.
- Costabel U. The changing treatment landscape in idiopathic pulmonary fibrosis. *Eur Respir Rev* 2015;24:65-8.
- Zhou J, Zhang HA, Lin Y, Liu HM, Cui YM, Xu Y, Zhao N, Ma JM, Fan K, Jiang CL. Protective effect of ginsenoside against acute renal failure via reduction of renal oxidative stress and enhanced expression of ChAT in the proximal convoluted tubule and ERK1/2 in the paraventricular nuclei. *Physiol Res* 2014;63:597-604.
- Kamel EO, Hady AARA, Abd Elrahman ASAH, Diab MM. Evaluation of role of captopril and erdosteine in protection of the lung against bleomycin-induced injury in rats. *Egypt J Hosp Med* 2019;75:1937-45.
- Ma H, Jo YJ, Ma Y, Hong JT, Kwon BM, Oh KW. Obovatol isolated from *Magnolia obovata* enhances pentobarbital-induced sleeping time: possible involvement of GABAA receptors/chloride channel activation. *Phytomedicine* 2009;16:308-13.
- Bancroft JD, Layton C. The hematoxylin and eosin. In: Suvarna SK, Layton C, Bancroft JD, editors. *Bancroft's Theory and*

- Practice of Histological Techniques. 8th ed. London: Elsevier; 2019. p.126-38.
26. Kiernan JA. Histological and histochemical methods: theory and practice. 5th ed. Banbury: Scion; 2015.
 27. Sanderson T, Wild G, Cull AM, Marston J, Zardin G. Immunohistochemical and immunofluorescent techniques. In: Suvarna SK, Layton C, Bancroft JD, editors. Bancroft's Theory and Practice of Histological Techniques. 8th ed. London: Elsevier; 2019. p.337-94.
 28. Woods AE, Stirling JW. Transmission electron microscopy. In: Suvarna SK, Layton C, Bancroft JD, editors. Bancroft's Theory and Practice of Histological Techniques. 8th ed. London: Elsevier; 2019. p.434-75.
 29. Beauchamp C, Fridovich I. Superoxide dismutase: improved assays and an assay applicable to acrylamide gels. *Anal Biochem* 1971;44:276-87.
 30. Sinha AK. Colorimetric assay of catalase. *Anal Biochem* 1972;47:389-94.
 31. Ohkawa H, Ohishi N, Yagi K. Assay for lipid peroxides in animal tissues by thiobarbituric acid reaction. *Anal Biochem* 1979;95:351-8.
 32. Rosner B. Fundamentals of biostatistics. 8th ed. Boston: Cengage Learning; 2015.
 33. Bilgin G, Kismet K, Kuru S, Kaya F, Senes M, Bayrakceken Y, Yumusak N, Celikkan FT, Erdemli E, Celemlı OG, Sorkun K, Koca G. Ultrastructural investigation of the protective effects of propolis on bleomycin induced pulmonary fibrosis. *Biotech Histochem* 2016;91:195-203.
 34. Dong SH, Liu YW, Wei F, Tan HZ, Han ZD. Asiatic acid ameliorates pulmonary fibrosis induced by bleomycin (BLM) via suppressing pro-fibrotic and inflammatory signaling pathways. *Biomed Pharmacother* 2017;89:1297-309.
 35. Arezzini B, Vecchio D, Signorini C, Stringa B, Gardi C. F2-isoprostanes can mediate bleomycin-induced lung fibrosis. *Free Radic Biol Med* 2018;115:1-9.
 36. Jang SS, Kim HG, Han JM, Lee JS, Choi MK, Huh GJ, Son CG. Modulation of radiation-induced alterations in oxidative stress and cytokine expression in lung tissue by Panax ginseng extract. *Phytother Res* 2015;29:201-9.
 37. Altintas N, Erboga M, Aktas C, Bilir B, Aydin M, Sengul A, Ates Z, Topcu B, Gurel A. Protective effect of infliximab, a tumor necrosis factor- α inhibitor, on bleomycin-induced lung fibrosis in rats. *Inflammation* 2016;39:65-78.
 38. Tian SL, Yang Y, Liu XL, Xu QB. Emodin attenuates bleomycin-induced pulmonary fibrosis via anti-inflammatory and anti-oxidative activities in rats. *Med Sci Monit* 2018;24:1-10.
 39. Tang H, Gao L, Mao J, He H, Liu J, Cai X, Lin H, Wu T. Salidroside protects against bleomycin-induced pulmonary fibrosis: activation of Nrf2-antioxidant signaling, and inhibition of NF- κ B and TGF- β 1/Smad-2/-3 pathways. *Cell Stress Chaperones* 2016;21:239-49.
 40. Mazzoli-Rocha F, Carvalho GM, Lanzetti M, Valena SS, Silva LF, Saldiva PH, Zin WA, Faffe DS. Respiratory toxicity of repeated exposure to particles produced by traffic and sugar cane burning. *Respir Physiol Neurobiol* 2014;191:106-13.
 41. Rago F, Melo EM, Kraemer L, Galvo I, Cassali GD, Santos RAS, Russo RC, Teixeira MM. Effect of preventive or therapeutic treatment with angiotensin 1-7 in a model of bleomycin-induced lung fibrosis in mice. *J Leukoc Biol* 2019;106:677-86.
 42. Li L, Li D, Xu L, Zhao P, Deng Z, Mo X, Li P, Qi L, Li J, Gao J. Total extract of Yupingfeng attenuates bleomycin-induced pulmonary fibrosis in rats. *Phytomedicine* 2015;22:111-9.
 43. Meng L, Zhang X, Wang H, Dong H, Gu X, Yu X, Liu Y. Yangyin Yiqi Mixture ameliorates Bleomycin-induced pulmonary fibrosis in rats through inhibiting TGF- β 1/Smad pathway and epithelial to mesenchymal transition. *Evid Based Complement Alternat Med* 2019;2019:2710509.
 44. Chen F, Wang PL, Fan XS, Yu JH, Zhu Y, Zhu ZH. Effect of Renshen Pingfei Decoction, a traditional Chinese prescription, on IPF induced by Bleomycin in rats and regulation of TGF- β 1/Smad3. *J Ethnopharmacol* 2016;186:289-97.
 45. Tawfik MK, Makary S. 5-HT7 receptor antagonism (SB-269970) attenuates bleomycin-induced pulmonary fibrosis in rats via downregulating oxidative burden and inflammatory cascades and ameliorating collagen deposition: comparison to terguride. *Eur J Pharmacol* 2017;814:114-23.
 46. Liu J, Han Z, Han Z, He Z. Mesenchymal stem cell-conditioned media suppresses inflammation-associated overproliferation of pulmonary artery smooth muscle cells in a rat model of pulmonary hypertension. *Exp Ther Med* 2016;11:467-75.
 47. Zaaan MA, Zaki HF, El-Brairy AI, Kenawy SA. Pyrrolidinedithiocarbamate attenuates bleomycin-induced pulmonary fibrosis in rats: modulation of oxidative stress, fibrosis, and inflammatory parameters. *Exp Lung Res* 2016;42:408-16.
 48. Zuo WL, Zhao JM, Huang JX, Zhou W, Lei ZH, Huang YM, Huang YF, Li HG. Effect of bosentan is correlated with MMP-9/TIMP-1 ratio in bleomycin-induced pulmonary fibrosis. *Biomed Rep* 2017;6:201-5.
 49. Goto K, Imaoka M, Goto M, Kikuchi I, Suzuki T, Jindo T, Takasaki W. Effect of body-weight loading onto the articular cartilage on the occurrence of quinolone-induced chondrotoxicity in juvenile rats. *Toxicol Lett* 2013;216:124-9.
 50. Li Y, Wang S, Wang Y, Zhou C, Chen G, Shen W, Li C, Lin W, Lin S, Huang H, Liu P, Shen X. Inhibitory effect of the anti-malarial agent artesunate on collagen-induced arthritis in rats through nuclear factor kappa B and mitogen-activated protein kinase signaling pathway. *Transl Res* 2013;161:89-98.
 51. Li Q, Mao M, Qiu Y, Liu G, Sheng T, Yu X, Wang S, Zhu D. Key role of ROS in the process of 15-lipoxygenase/15-hydroxyeicosatetraenoic acid-induced pulmonary vascular remodeling in hypoxia pulmonary hypertension. *PLoS One* 2016;11:e0149164.
 52. Chen Q, Wang Q, Zhu J, Xiao Q, Zhang L. Reactive oxygen species: key regulators in vascular health and diseases. *Br J Pharmacol* 2018;175:1279-92.
 53. Verma R, Kushwah L, Gohel D, Patel M, Marvania T, Balakrishnan S. Evaluating the ameliorative potential of quercetin against the bleomycin-induced pulmonary fibrosis in Wistar rats. *Pulm Med* 2013;2013:921724.

54. Sabry M, Taha HH, Mohamed AO, Thabet K, Hasan AA, Abdel-Razik ARH, Elsayed BEM. TLR4/NF- κ B signaling pathway is a key pathogenic event of lung injury in bleomycin-induced pulmonary fibrosis in a mouse model. *Az J Pharm Sci* 2020;61:92-103.
55. Kato S, Inui N, Hakamata A, Suzuki Y, Enomoto N, Fujisawa T, Nakamura Y, Watanabe H, Suda T. Changes in pulmonary endothelial cell properties during bleomycin-induced pulmonary fibrosis. *Respir Res* 2018;19:127.
56. Kim MS, Kim SH, Jeon D, Kim HY, Lee K. Changes in expression of cytokines in polyhexamethylene guanidine-induced lung fibrosis in mice: Comparison of bleomycin-induced lung fibrosis. *Toxicology* 2018;393:185-92.
57. Fanny M, Nascimento M, Baron L, Schricke C, Maillat I, Akbal M, Riteau N, Le Bert M, Quesniaux V, Ryffel B, Gombault A, Mème S, Mème W, Couillin I. The IL-33 receptor ST2 regulates pulmonary inflammation and fibrosis to bleomycin. *Front Immunol* 2018;9:1476.
58. Zhao L, Mu B, Zhou R, Cheng Y, Huang C. Igaratimod ameliorates bleomycin-induced alveolar inflammation and pulmonary fibrosis in mice by suppressing expression of matrix metalloproteinase-9. *Int J Rheum Dis* 2019;22:686-94.
59. Comeglio P, Filippi S, Sarchielli E, Morelli A, Cellai I, Corno C, Pini A, Adorini L, Vannelli GB, Maggi M, Vignozzi L. Therapeutic effects of obeticholic acid (OCA) treatment in a bleomycin-induced pulmonary fibrosis rat model. *J Endocrinol Invest* 2019;42:283-94.
60. Shamskhou EA, Kratochvil MJ, Orcholski ME, Nagy N, Kaber G, Steen E, Balaji S, Yuan K, Keswani S, Danielson B, Gao M, Medina C, Nathan A, Chakraborty A, Bollyky PL, De Jesus Perez VA. Hydrogel-based delivery of Il-10 improves treatment of bleomycin-induced lung fibrosis in mice. *Biomaterials* 2019;203:52-62.
61. Okamoto A, Nojiri T, Konishi K, Tokudome T, Miura K, Hosoda H, Hino J, Miyazato M, Kyomoto Y, Asai K, Hirata K, Kangawa K. Atrial natriuretic peptide protects against bleomycin-induced pulmonary fibrosis via vascular endothelial cells in mice: ANP for pulmonary fibrosis. *Respir Res* 2017;18:1.
62. Kabel AM, Omar MS, Elmaaboud MAA. Amelioration of bleomycin-induced lung fibrosis in rats by valproic acid and butyrate: Role of nuclear factor kappa-B, proinflammatory cytokines and oxidative stress. *Int Immunopharmacol* 2016;39:335-42.
63. Mulero MC, Wang VY, Huxford T, Ghosh G. Genome reading by the NF- κ B transcription factors. *Nucleic Acids Res* 2019;47:9967-89.
64. Serasanambati M, Chilakapati SR. Function of nuclear factor kappa B (NF- κ B) in human diseases- a review. *South Indian J Biol Sci* 2016;2:368-87.
65. Tilborghs S, Corthouts J, Verhoeven Y, Arias D, Rolfo C, Trinh XB, van Dam PA. The role of Nuclear Factor-kappa B signaling in human cervical cancer. *Crit Rev Oncol Hematol* 2017;120:141-50.
66. Qin X, Yan M, Wang X, Xu Q, Wang X, Zhu X, Shi J, Li Z, Zhang J, Chen W. Cancer-associated fibroblast-derived IL-6 promotes head and neck cancer progression via the Osteopontin-NF-kappa B signaling pathway. *Theranostics* 2018;8:921-40.
67. Wu J, Ding J, Yang J, Guo X, Zheng Y. MicroRNA roles in the nuclear factor kappa B signaling pathway in cancer. *Front Immunol* 2018;9:546.
68. Alvira CM. Nuclear factor-kappa-B signaling in lung development and disease: one pathway, numerous functions. *Birth Defects Res A Clin Mol Teratol* 2014;100:202-16.
69. Hou J, Ma T, Cao H, Chen Y, Wang C, Chen X, Xiang Z, Han X. TNF- α -induced NF- κ B activation promotes myofibroblast differentiation of LR-MSCs and exacerbates bleomycin-induced pulmonary fibrosis. *J Cell Physiol* 2018;233:2409-19.
70. Taooka Y. Neutrophil-mediated lung diseases and integrin α subfamily, α 4 and α 9. *J Respir Res* 2017;3:95-7.
71. Li G, Jin F, Du J, He Q, Yang B, Luo P. Macrophage-secreted TSLP and MMP9 promote bleomycin-induced pulmonary fibrosis. *Toxicol Appl Pharmacol* 2019;366:10-6.
72. Tamò L, Simillion C, Hibaoui Y, Feki A, Gugger M, Prasse A, Jäger B, Goldmann T, Geiser T, Gazdhar A. Gene network analysis of interstitial macrophages after treatment with induced pluripotent stem cells secretome (iPSC-cm) in the bleomycin injured rat lung. *Stem Cell Rev Rep* 2018;14:412-24.
73. Kandhare AD, Bodhankar SL, Mohan V, Thakurdesai PA. Effect of glycosides based standardized fenugreek seed extract in bleomycin-induced pulmonary fibrosis in rats: decisive role of Bax, Nrf2, NF- κ B, Muc5ac, TNF- α and IL-1 β . *Chem Biol Interact* 2015;237:151-65.
74. Zhao Q, Wu J, Lin Z, Hua Q, Zhang W, Ye L, Wu G, Du J, Xia J, Chu M, Hu X. Resolvin D1 alleviates the lung ischemia reperfusion injury via complement, immunoglobulin, TLR4, and inflammatory factors in rats. *Inflammation* 2016;39:1319-33.
75. Zhou Z, Kandhare AD, Kandhare AA, Bodhankar SL. Hesperidin ameliorates bleomycin-induced experimental pulmonary fibrosis via inhibition of TGF-beta1/Smad3/AMPK and I κ B/NF-kappaB pathways. *EXCLI J* 2019;18:723-45.
76. Hüttemann M, Helling S, Sanderson TH, Sinkler C, Samavati L, Mahapatra G, Varughese A, Lu G, Liu J, Ramzan R, Vogt S, Grossman LI, Doan JW, Marcus K, Lee I. Regulation of mitochondrial respiration and apoptosis through cell signaling: cytochrome c oxidase and cytochrome c in ischemia/reperfusion injury and inflammation. *Biochim Biophys Acta* 2012;1817:598-609.
77. Liu X, Chen Z. The pathophysiological role of mitochondrial oxidative stress in lung diseases. *J Transl Med* 2017;15:207.
78. Burman A, Tanjore H, Blackwell TS. Endoplasmic reticulum stress in pulmonary fibrosis. *Matrix Biol* 2018;68-69:355-65.
79. Arafa MH, Mohamed DA, Atteia HH. Ameliorative effect of N-acetyl cysteine on alpha-cypermethrin-induced pulmonary toxicity in male rats. *Environ Toxicol* 2015;30:26-43.
80. El-Khouly D, El-Bakly WM, Awad AS, El-Mesallamy HO, El-Demerdash E. Thymoquinone blocks lung injury and fibrosis by attenuating bleomycin-induced oxidative stress and activation of nuclear factor Kappa-B in rats. *Toxicology* 2012;302:106-13.

81. Bahri S, Ben Ali R, Gasmi K, Mlika M, Fazaa S, Ksouri R, Seirairi R, Jameleddine S, Shlyonsky V. Prophylactic and curative effect of rosemary leaves extract in a bleomycin model of pulmonary fibrosis. *Pharm Biol* 2017;55:462-71.
82. Gao Y, Yao LF, Zhao Y, Wei LM, Guo P, Yu M, Cao B, Li T, Chen H, Zou ZM. The Chinese herbal medicine formula mKG suppresses pulmonary fibrosis of mice induced by bleomycin. *Int J Mol Sci* 2016;17:238.
83. Zhou Y, Liao S, Zhang Z, Wang B, Wan L. Astragalus injection attenuates bleomycin-induced pulmonary fibrosis via down-regulating Jagged1/Notch1 in lungs. *J Pharm Pharmacol* 2016;68:389-96.
84. Saba E, Jeon BR, Jeong DH, Lee K, Goo YK, Kwak D, Kim S, Roh SS, Kim SD, Nah SY, Rhee MH. A novel Korean red ginseng compound gintonin inhibited inflammation by MAPK and NF- κ B pathways and recovered the levels of mir-34a and mir-93 in RAW 264.7 cells. *Evid Based Complement Alternat Med* 2015;2015:624132.
85. Ahn S, Singh P, Castro-Aceituno V, Yesmin Simu S, Kim YJ, Mathiyalagan R, Yang DC. Gold nanoparticles synthesized using Panax ginseng leaves suppress inflammatory - mediators production via blockade of NF- κ B activation in macrophages. *Artif Cells Nanomed Biotechnol* 2017;45:270-6.
86. Ren J, Wang LX, Ji XC, Zhou JY, Zhang MY. Ultrastructural observation on pulmonary fibrosis in E9 rats treated with compound Carapax trionycis formula. *Asian Pac J Trop Med* 2013;6:153-5.
87. Im K, Kim J, Min H. Ginseng, the natural effectual antiviral: Protective effects of Korean Red Ginseng against viral infection. *J Ginseng Res* 2016;40:309-14.
88. Hsieh YH, Deng JS, Chang YS, Huang GJ. Ginsenoside Rh2 ameliorates lipopolysaccharide-induced acute lung injury by regulating the TLR4/PI3K/Akt/mTOR, Raf-1/MEK/ERK, and Keap1/Nrf2/HO-1 signaling pathways in mice. *Nutrients* 2018;10:1208.
89. Hafez MM, Hamed SS, El-Khadragy MF, Hassan ZK, Al Rejaie SS, Sayed-Ahmed MM, Al-Harbi NO, Al-Hosaini KA, Al-Harbi MM, Alhoshani AR, Al-Shabanah OA, Alsharari SD. Effect of ginseng extract on the TGF- β 1 signaling pathway in CCl₄-induced liver fibrosis in rats. *BMC Complement Altern Med* 2017;17:45.
90. Mansour HH. Protective effect of ginseng against gamma-irradiation-induced oxidative stress and endothelial dysfunction in rats. *EXCLI J* 2013;12:766-77.
91. Zhang XH, Xu XX, Xu T. Ginsenoside Ro suppresses interleukin-1 β -induced apoptosis and inflammation in rat chondrocytes by inhibiting NF- κ B. *Chin J Nat Med* 2015;13:283-9.
92. Rastogi V, Santiago-Moreno J, Doré S. Ginseng: a promising neuroprotective strategy in stroke. *Front Cell Neurosci* 2015;8:457.
93. Duguran DR, Lopez MJC, Valenzuela MTCE, Ples MB, Vitor II RJS. Protective potential of ginseng and silymarin on the liver and kidney of ethanol-treated mice (*Mus musculus*). *Natl J Physiol Pharm Pharmacol* 2018;8:969-76.